A DNP-NMR setup for sub-nanoliter samples

Pedro Freire da Silva, Supervisor(s): Prof. Giovanni Boero, Prof. Pedro Sebastião

The electrical and mechanical design for a non-magnetic, 2.5x2.5 cm^2 setup with µm-precision, along with 1.0x10 cm^2 optimized probes, was simulated and implemented to perform simultaneously EPR and DNP-NMR studies. The interaction coils were EM-FEM modelled and verified against optimized EPR and NMR experimental results for sub-nL samples of water, PDMS and TEMPO. DNP state-of-the-art, theory and future prospects were also presented.

I Introduction

Nuclear magnetic resonance (NMR) detection is a widespread technique use in a variety of fields both in spectroscopy and imaging that primes for its chemical insight, selectiveness and non-invasive behaviour[1]. Its main downside is the sharp dependence on magnetic field strength and sample size, meaning sensitivity has proven to be the limiting factor to the wider use of this technique. Another common limitation is the difficult use of the technique for low gyromagnetic ratio nuclei, namely the biological cornerstone that is ^{13}C, which shows a sensitivity 170 times smaller[2] than ^{1}H. This led to the development of complimentary techniques to achieve better resolution, in less time and with cheaper medium-field magnets, and that would allow for the study of more isotopes. These ranged from pulsed techniques to remove or insert interactions with other species (such as cross-polarizing ^{13}C to match the polarization of ^{1}H , CP-NMR[3], or the dipolar-dipolar decoupling that highly sharpens lines, through TROSY), to hyperpolarization techniques, such as the one implemented here, Dynamic Nuclear Polarization (DNP). Much like other cross-polarization techniques, DNP hyperpolarizes the nuclei up to the thermal polarization of the electrons, which means an increase of approximately 660 in signal or over 400 000 less time averaging out the noise. This technique was implemented, at a field of 0.7 T, to mass-limited samples in the sub-nL range, which mean a signal over a 10^8 times smaller than regular samples and medium fields, using a versatile and low cost 3D-printed setup.

II Theory and simulations

The spectroscopic analysis of such a small sample requires a far higher spin sensitivity as that of regular systems, achieved with small detection coils for a high filling factor of the volume used, and low noise designs. These were used from published designs[4,5] with 130 CMOS printed coils and integrated electronics to achieve the highest possible SNR. The following equation states the dependences taken into consideration when the system was developed[2]:

$$\mathrm{SNR} \propto \varepsilon\,\eta\,\frac{{B_0}^{7/4}\gamma^{11/4}}{T_S}\langle B_{1\perp}\sin(\gamma\tau B_{1\perp})\rangle \qquad (1)$$

for a filling factor η, unitary field produced by the detection coil $B_{1\perp}$ perpendicularly to the fixed magnetic field B_0, sample temperature T_S and gyromagnetic ratio γ and all for a DNP enhancement of ε, proportional to $B_{1\perp EPR}^2$.

It was thus necessary to analyze all the magnetic fields at play, the one created by the NMR coil, the unitary field, and the DNP-generating field created by the EPR coil repurposed for this experiment. This was done through FEM in COMSOL Multiphysics, solving the Maxwell equations for the geometry designed in Solidworks, exactly as used in the real setup and the working NMR/EPR frequencies at ~1 T. This allowed for an understanding of the geometrical restrictions created by the small sensitive volume of each coil and therefore of the necessity for a precise system, with losses per deviation, in the sensitive volume, of around 50%/20 µm. The same simulation allowed for the study and future optimization of the dielectric heating of the sample.

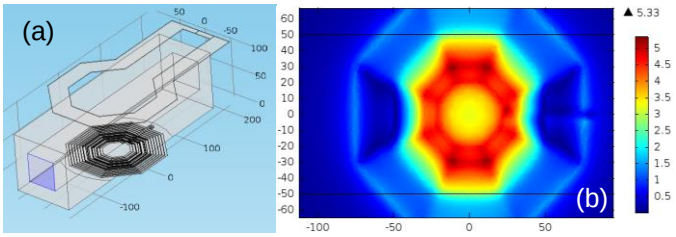

Fig 1- Geometry simulated in Solidworks and imported into COMSOL (a) and transversal unitary magnetic field in the xy plane on the bottom of the capillary (b). Dimensions in µm and magnetic field in Gauss.

The desired DNP enhancement is based is based on relaxations effects of the excited polarization after microwave irradiation, which depend on cross-relaxation and auto-relaxations factors σ and ρ, respectively, as:

$$\frac{d\langle I_z\rangle}{dt} = -\rho(\langle I_z\rangle - I_0) - \sigma(\langle S_z\rangle - S_0) \qquad (2)$$

This equation can be rewritten to fit experimentally verifiable values such as the saturation factor s, the leakage factor f and the coupling factor ξ:

$$\varepsilon = \frac{\langle I_z\rangle}{I_0} = 1 - s\,\xi\,f\,\frac{|\gamma_e|}{\gamma_n} \qquad (3)$$

From these, the saturation factor is the only one that is dependent on the setup and not the sample used:

$$s = \frac{S_0 - \langle S_z\rangle}{S_0} \quad , \quad 1 - 660\,s \le \varepsilon_{exp} \le 1 + 330\,s \qquad (4)$$

And is thus proportional to the EPR excitation field squared and its proximity to the sample. Considering the SNR is proportional to the enhanced magnetization, that the signal is geometrically correlated to the unitary field in a point of space and that, for high enhancements, ε is proportional to the saturation factor created by the EPR coil's excitation ($660s \gg 1$):

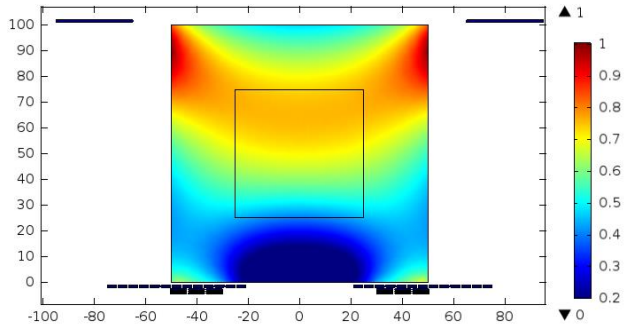

Fig 2- Normalized contribution to the total signal as deduced from $B^2_{1\perp EPR}B_{1\perp NMR}$, with the above considerations. Cross section shows the two coils and the 100x100 µm² capillary used. Dimensions in µm.

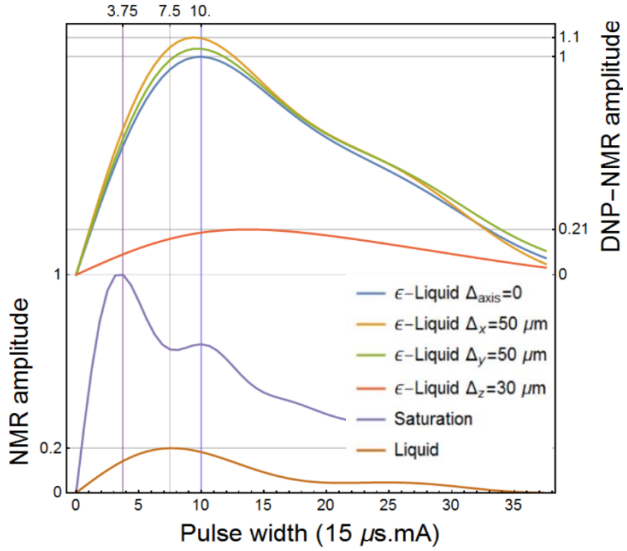

Fig 3- Relative amplitudes of NMR and DNP-NMR signals for different samples, in different spaces, with respect to RF pulse length. DNP-NMR comparison made normalized to axial alignment and capillary contact.

It was found that pulse length has a significant effect and must be optimized and that whereas a vertical displacement has induces a significant signal drop, on-plane shifts have little effect, even introducing a small increase, due to the larger size of the EPR coil.

A highly compact (2.5x2.5 cm²) design with micrometric precision and the ability to be inserted in commercial superconducting magnets was thus developed to perform EPR and NMR concurrently, possibly at cryogenic temperatures. The capillary modelled and shown above was used for ease (only introducing a factor of 0.2 relative to full sample occupation between coils), as this was a proof of principle design and the simulation framework was designed for later optimization.

The concurrent use of both hyperpolarization and detection spared the losses common in shuttling designs along *i* sites with the pre-polarization done in different magnet conditions:

$$\frac{\varepsilon}{\varepsilon_0} = \frac{T_{NMR}}{T_{EPR}}\frac{B_{EPR}}{B_{NMR}}\prod_i e^{-t_i/T_i} \qquad (5)$$

In which the small nuclear polarization times, usually in the 10-100 ms range, can be comparable to the shuttling times.

III Mechanical implementation

The mechanical design was fully developed in Solidworks and dimensioned through finite element simulations (FEM) targeting critical zones. A hard plastic with low thermal expansion coefficient was used, EX200, throughout the system with a printing tolerance of 50-100 µm.

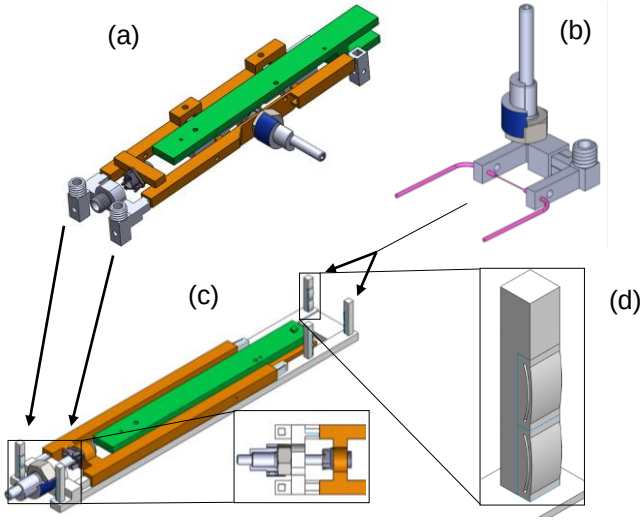

Fig 4- Solidworks model of the system. Table system for the EPR (a) and NMR (c) PCB's (in green), the microfluidic system (c) and detail of its attachment (d). Arrows indicate the correct placement of each part.

The precision requirements were achieved using locking pieces on all moving parts, as above in (d), modelled to act as springs, thus reducing the possible moving room from up to 100 µm to zero. The control along an axis is done with an attachable piece (through an M6 nut/thread system) containing a magnetic micrometric screw.

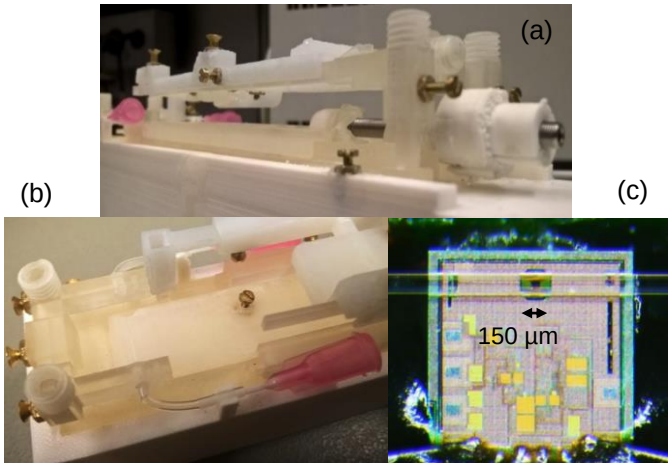

Fig 5- Final prototype seen from the back (a) and the front (b). M1.6 screws used to control friction and to lock movement are shown as well as the adjustment system and capillary interface. Image of the precision achieved when aligning the capillary with the NMR coil (c)

IV Electrical implementation

To interface the NMR and EPR microchips, two compact PCB's were designed in a configuration that would allow for contact of the two despite the space introduced by the *Al* wedge-wedge and *Au* ball-wedge wirebonding as subsequent epoxy cover layer.

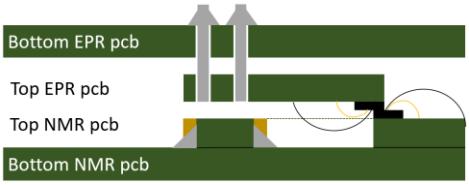

Fig 6- Schematic of the assembly of the PCB's when aligned. Bottom PCB's are 10x1 cm^2 and top ones are 2x1 (EPR) and 3x1 (NMR) cm^2.

The EPR PCB required only DC inputs which were filtered or generated by an LDO on the PCB. The two symmetric outputs, in the 500 MHz range, were subtracted, band-pass filtered between 100-1000 MHz and outputted through an SMA cable soldered directly on the PCB. The top PCB connected contained only DC filtering.

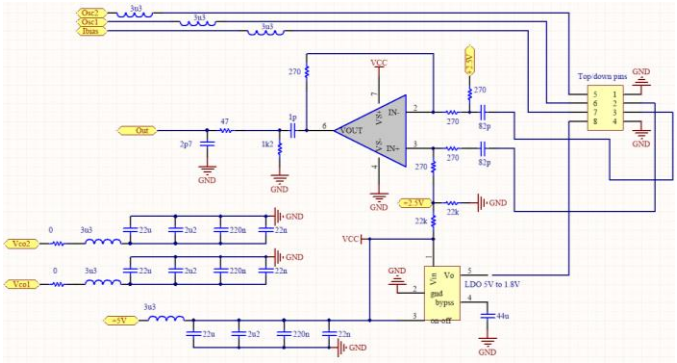

Fig 7- Schematic of the EPR PCB up to the top/bottom pins.

The NMR PCB was fed by 5V with Tx and Rx voltages being generated by LDO's, filtered and used to feed the TTL inverter to control the digital operation toggling pulse.

It also required an RF excitation biased using a Bias Tee design and, when the same frequency is used for downconversion and RF excitation, an R to 2R network. Otherwise the lines would simply be separated and ESD protected by back-to-back diodes. The output was in the kHz range and biased at 1V. A protection voltage follower was used before it being amplified with a gain of 10. The design was a non-inverting OPAMP working at a 1 V virtual ground, made through a voltage divider from the highly capacitor-filtered VCC line feeding a higher impedance OPAMP feedback loop.

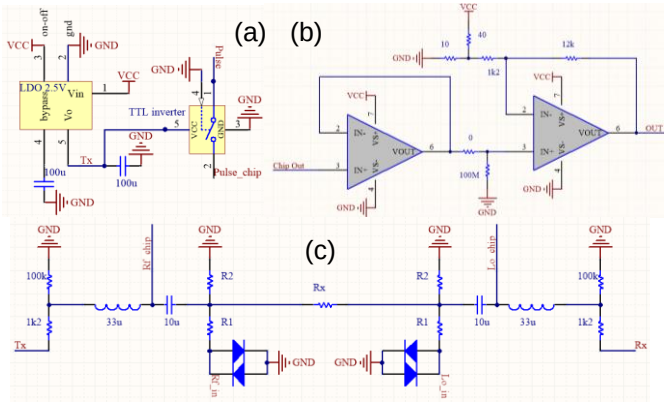

Fig 8- Schematic of the NMR PCB's power management (a), output stage (b) and excitation/downconversion RF input stage (c).

V Results and conclusions

After assembly and testing samples of water, PDMS and 50/200 mM TEMPO were used to optimize experimental parameters, such as NMR downconversion frequency and the exponential filter's characteristic time or the maximum EPR modulation past which one would saturate the lock-in detector or broaden the linewidth. Selected results are shown in figure 10. The simulation results were then double checked experimentally and the optimal pulse length was found and used henceforth.

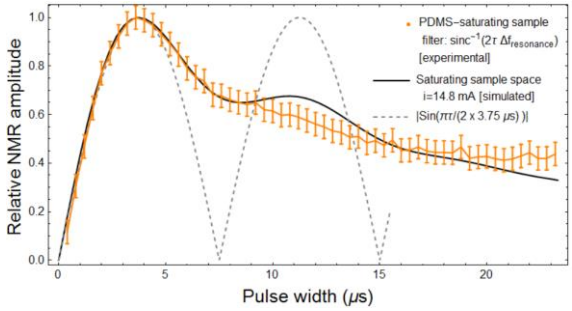

Fig 9- Comparison of experimental, simulated and theoretical, for a single spin, NMR amplitudes with respect to the time of the RF pulse.

Having assembled the circuit, it was aligned using a modulation of the NMR pulse control line, thus inducing the same modulation frequency on the EPR coil, which was adjusted until the maximum signal was achieved.

After this easy alignment procedure, the setup was introduced into the magnet and the EPR excitation line to be excited and DNP-studied was searched for. This was done through a field sweep and a return to the discovered excitation matching field. Due to the hysteresis of the electromagnet and to have control over the excited frequency, a second smaller sweep using the control voltages of the varactors was done, setting the resonance frequency.

Due to magnet malfunction, the DNP results were not yet obtained, but will serve a purpose on future developments of the technique be it coil integration, parallelization, post-CMOS microfabrication or as a complementary technique in a micro total analysis system, μTAS.

VI Acknowledgements

This project used the resources of LMIS1 at EPFL under the direct supervision of Dr. G. Boero and indirect from Dr. P. Sebastião. The aid and guidance of E. Montinaro, G. Gualco and M. Grisi was also highly appreciated.

VII Bibliography

1. Hore, P. J. *Nuclear Magnetic Resonance*. (Oxford University Press, 2015).

2. Hoult, D. . & Richards, R. . The signal-to-noise ratio of the nuclear magnetic resonance experiment. *J. Magn. Reson.* **24,** 71–85 (1976).

3. Stejskal, E. ., Schaefer, J. & Waugh, J. . Magic-angle spinning and polarization transfer in proton-enhanced NMR. *J. Magn. Reson.* **28,** 105–112 (1977).

4. Grisi, M., Gualco, G. & Boero, G. A broadband single-chip transceiver for multi-nuclear NMR probes. *Rev. Sci. Instrum.* **86,** 044703 (2015).

5. Gualco, G. *et al.* Cryogenic single-chip electron spin resonance detector. *J. Magn. Reson.* **247,** 96–103 (2014).

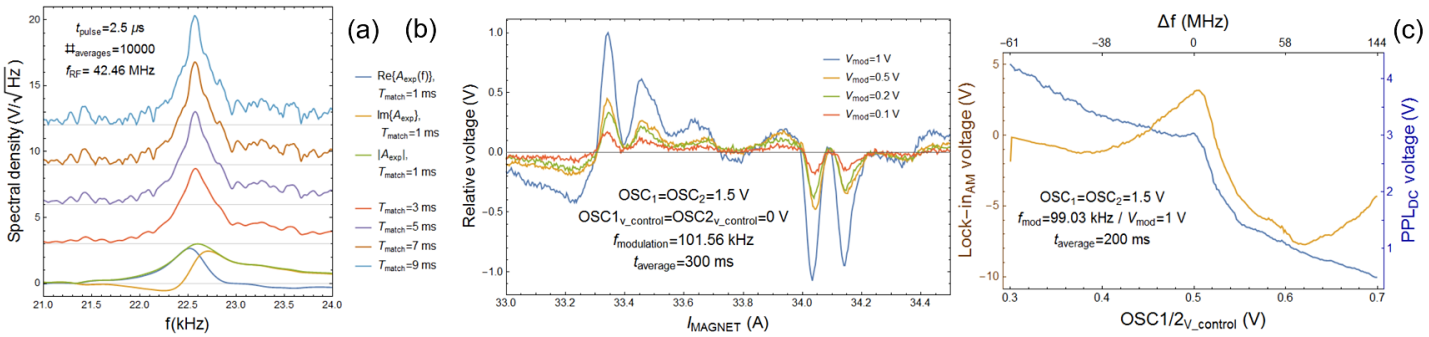

Fig 10- NMR for PDMS at different characteristic times for an exponential filter (a) ,EPR results for 50 mM TEMPO at different field-modulations using a field sweep (b) and for 200 Mm TEMPO using a controlled sweep of the VCO's oscillation frequency (c). Experimental conditions described on the pictures.